Journal of Visualization, Vol. 5, No. 1 (2002) 77-84

# PIV Measurements of Side-Cavity Open-Channel Flows — Wando Model in Rivers —

Nezu, I.* and Onitsuka, K.*

* Department of Civil & Global Environment Engineering, Kyoto University, Yoshidahonmachi, Sakyo-ku, Kyoto 606-8501, Japan.

Received 8 August 2001.
Revised 29 October 2001.

***Abstract*:** PIV measurements in side-cavity open-channel flows that simulate "Wando" in rivers, were conducted in a laboratory flume. Five types of side cavities were built by using a transparent plate at the wando flow. The pattern of the instantaneous flow fields was quite different from that of time-averaged ones. It was found that a vortex, which is located in the side cavity, is stable when the junction mouth between the side-cavity and main channel is narrow. In contrast, large-scale unstable vortices are generated semi-periodically when the junction mouth is wide. The free-surface fluctuations in and outside the wando were also measured by three sets of supersonic wave gauges. The amplitude of the water-surface fluctuations is large when the junction mouth is wide as compared with when its mouth is narrow. When the elevation of the free surface in the side-cavity is rising, its elevation in the main channel is falling, and vice versa when the junction mouth is wide.

***Keywords*:** PIV, environmental hydraulics, wando flow, large-scale vortex, free surface.

## 1. Introduction

A lot of side-cavity open-channel flows can be observed at the riverbank in some Japanese rivers. Such a side-cavity is called "Wando" in river engineering, e.g., see Fig.1. Wando flow is very important in ecosystems as well as river engineering. Coherent horizontal vortices are generated by the shear instability between the main channel and the wando. Water-surface fluctuations near the spur dikes were measured by Chen and Ikeda (1996) and Ikeda et al. (1999) by using a water-wave gauge. They have shown that the frequency of vortices decreases downstream because some vortices coalesce with each other. Kimura et al. (1997) have found that an amplitude of water-surface fluctuations in a wando increases with an increase in the Froude number. Muto et al. (2000) measured two cases of wando with a laser Doppler anemometer (LDA) and flow visualization technique. The aspect ratio, which is a ratio of the lateral length to the streamwise length of side cavity, was 1 and 5. They indicated a distribution of turbulence intensity around the wando. Nezu et al. (2000) have measured instantaneous velocity fields in wando with the aspect ratio of 2, 3, 5 and 10 by using PIV. They investigated an evolution process of vortices which are generated near the junction.

Most researchers have investigated only simple concave side-cavity. In actual rivers, however, there are many shapes of side cavity. In this study, five types of wando were built by using a transparent plate in a straight glass flume. Turbulence measurements in and around side-cavity were conducted using PIV and three sets of supersonic water-wave gauges.

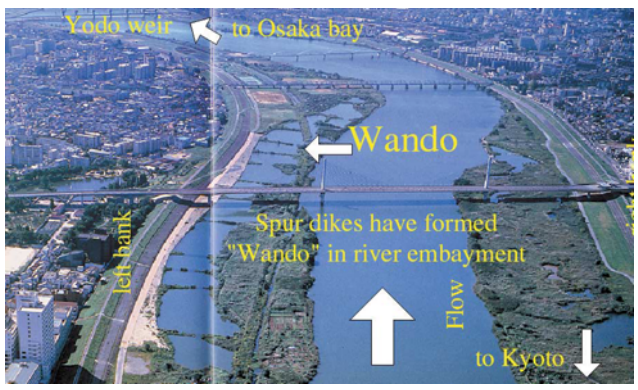


Fig. 1. Photo of Wando in Yodo River near the Yodo Weir.

## 2. Experimental Setup and Hydraulic Condition

The experiments were conducted in a 10 m long and 30 cm deep tilting flume, as shown in Fig. 2. Five types of side-cavities were built by the use of transparent plate, as shown in Fig. 3. $H$ is the water depth, $B_w$ is the spanwise length of wando, $L$ is the streamwise length of wando and $L_p$ is the length of the partition plate (see Fig. 2). Case A05 has no partition plate between the wando and the main channel. The partition plate is located at the upstream of wando in B05 ($L_p/L$ = 1/3) and C05 ($L_p/L$ = 2/3). In contrast, the partition plate is set at the downstream of wando in D05 ($L_p/L$ = 1/3) and E05 ($L_p/L$ = 2/3). Hydraulic conditions are summarized in Table 1. $Fr \equiv U_m/\sqrt{gH}$ is the Froude number and $U_m$ is the bulk mean velocity.

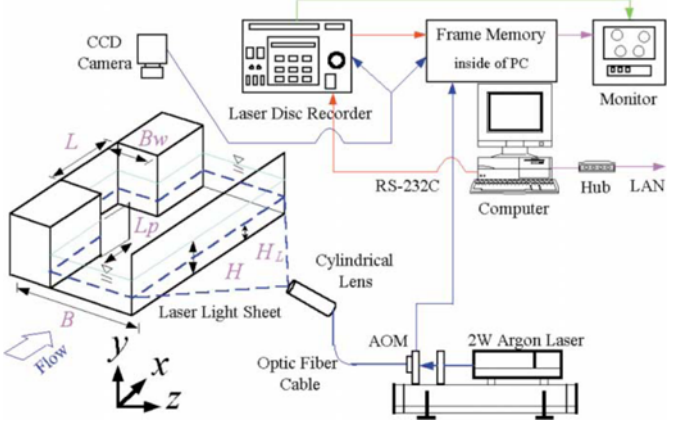


Fig. 2. Experimental set-up.

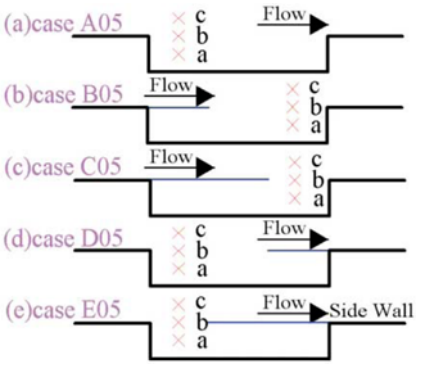


Fig. 3. Shape of five types of wando and measuring points of water surface fluctuations.

Table. 1. Hydraulic conditions.

| case | $H$ (cm) | $B_w$ (cm) | $L$ (cm) | $L/B_w$ | $L_p$ (cm) | $L_p/L$ | $Fr$ |
|---|---|---|---|---|---|---|---|
| A05 | | | | | - | - | |
| B05 | | | | | 6.7 | 0.34 | |
| C05 | 4.0 | 4.0 | 20.0 | 5.0 | 13.3 | 0.67 | 0.49 |
| D05 | | | | | 6.7 | 0.34 | |
| E05 | | | | | 13.3 | 0.67 | |

The PIV particles (Nylon-12: about 100 $\mu$m diameter and 1.02 specific density) were uniformly scattered in the circulating water of the flume. A 2W Argon-ion laser beam was guided through an optic-fiber cable and

illuminated horizontally through the glass side-wall as a 2 mm thickness laser light sheet (LLS) as shown in Fig. 2. A pair of images of tracer particles was taken in every 1/30 s step by a CCD camera which was placed above the channel. The pulse-wave period and its duration time were set to be 0.005 s and 0.001 s, respectively. The images were recorded on a laser disc by a laser disc recorder. These images which have 512 × 480 pixels were transferred then to a frame memory board inside of a personal computer. Instantaneous velocities in an image plane ($x$, $z$) were obtained by a cross correlation PIV algorithm including sub-pixel calculation. In the present study, the interrogation area was set to be 16 × 16 pixels. The cross correlation method may not be suitable for rotational flows consisting of small vortices. However, large-scale vortices can be described by this method. Nezu and Onitsuka (1998) and Nezu et al. (2000) have shown that the error of this PIV system is less than 3% in comparison with that of an LDA system. Furthermore, the free-surface fluctuations at three points (points a, b and c as shown in Fig. 3) for each case were measured by three sets of supersonic wave gauges.

# 3. Experimental Results and Discussions

## *3.1 Time-averaged Flow Fields*

Figure 4 shows the time-averaged velocity vector in all cases. In the case of A05, a long vortex, which has a streamwise scale $L$ and a spanwise scale $B_w$, can be seen in the wando. The center of the vortex is located near the downstream edge of the wando ($x/B_w \approx 4.5$). The velocity in the wando is much smaller than that in the main channel. In B05, a vortex is observed in the wando. It seems that there is no effect on the main channel because the direction of flow in the main channel is almost parallel to the $x$ direction.

In C05, two vortices are observed in the wando. One vortex, which is located in the lower reach, is generated by the shear instability between the main channel and the wando. The other vortex is seen in the upper reach. The velocity of the upper vortex is smaller than that of the lower one. The upper vortex may be generated by

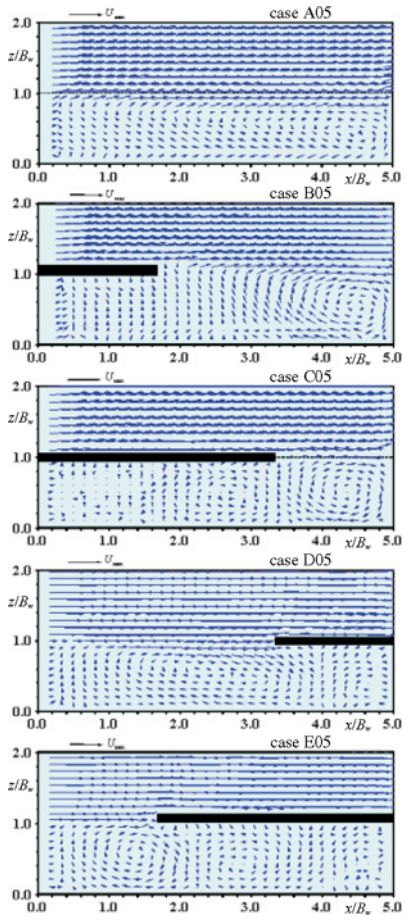


Fig. 4. Time-averaged flow fields.

the lower one, because there is no supply of momentum from the main channel just behind the partition plate. In D05, there are also two vortices. The rotations of these two vortices are in the opposite direction. The vortex in the upper reach is located in the junction mouth of the wando ($0 < x/B_w < 3.3$). A small-scale vortex is generated behind the partition plate by this upper vortex. The shape of this wando is symmetrical to the type of B05. However, the pattern of the vortex is quite different from each other. In E05, a pair of vortex is observed side by side near the junction mouth and behind the partition plate, respectively. Further, a small vortex is seen, but not so clear in the zone of $4.0 < x/B_w < 5.0$. The velocity of this small vortex is quite smaller than the other two vortices.

### *3.2 Instantaneous Flow Fields*

Figure 5 shows the instantaneous flow fields in all cases. In the case of A05, vortices are generated semi-periodically at the wando junction ($z/B_w = 1.0$) by a shear instability between the main channel and the wando. These vortices move downstream and grow up in scale. This is because the surrounding water is entrained by the coherent vortices. The pattern of these vortices is quite different from the time-averaged flow fields shown in Fig. 4.

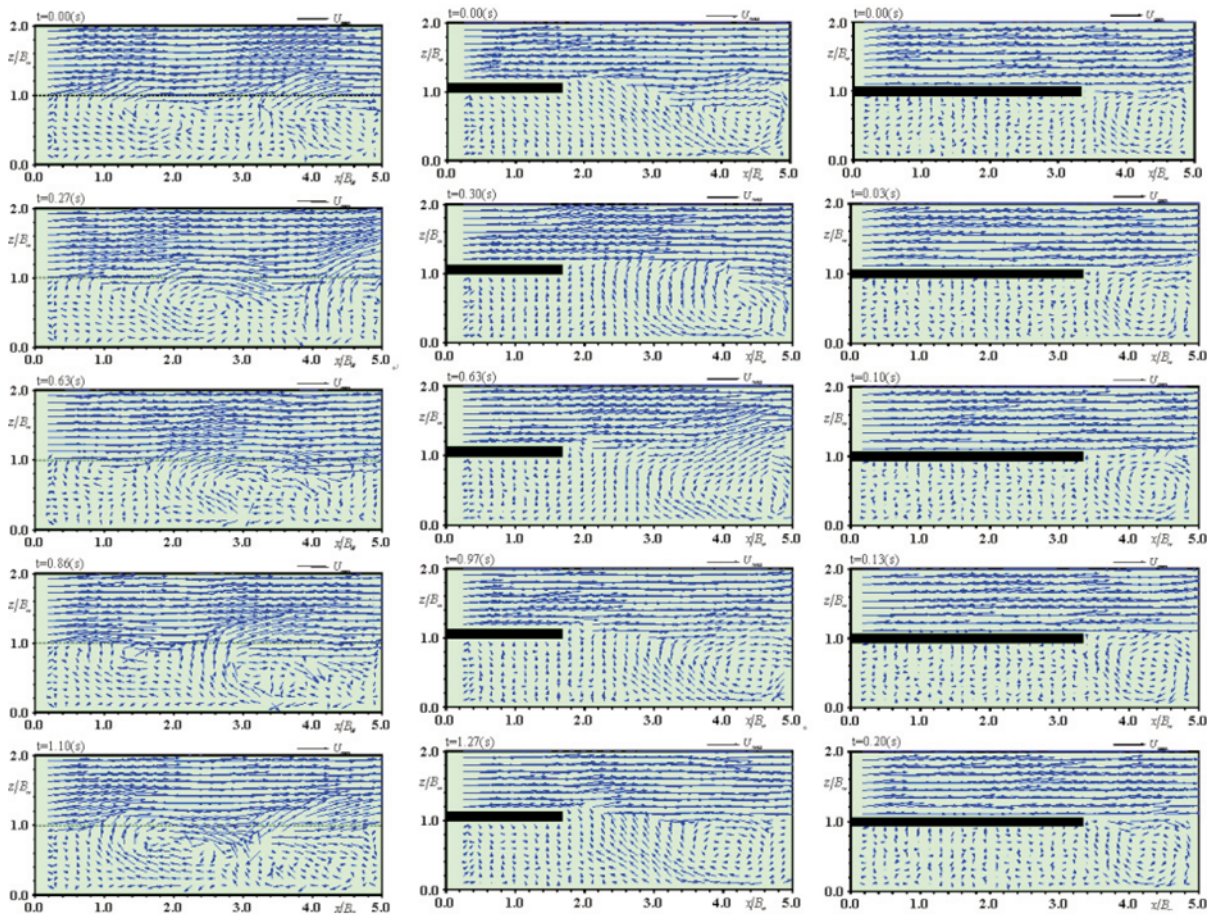


Fig. 5. Instantaneous flow fields.

In the case of B05, a large-scale vortex is generated in the wando ($2.0 < x/B_w < 5.0$). The water in the wando is sometimes transported toward the main channel by this vortex. This feature cannot be seen in the time-averaged fields shown in Fig. 4. The center of this vortex is a little moving in the wando. In contrast, the velocity behind the partition plate ($0 < x/B_w < 1.7$) is quite low in comparison with that of the large-scale vortex. The vector patterns at $t = 0.0$ s is similar in shape to those at $t = 1.27$ s. This period is evaluated from the FFT analysis of the velocity fluctuations. This implies that the period $T$ of the vortex appearance is about 1.3 s.

In the case of C05, a vortex is seen in the wando. The rotation speed of this vortex is smaller than that of the case B05. This vortex is more stable in comparison with that of the case B05. These characteristics in this case are similar to those of the wando with the aspect ratio (= $L/B_w$) of 3 which were obtained by Nezu et al. (2000).

In the case of D05, a strong flow parcel moves out from the wando toward the main channel at $t$ = 0.0 s. On the other hand, the flow parcel in the main channel moves into the wando at $t$ = 0.27 s and 0.57 s. As the results, a large-scale vortex is generated at $t$ = 0.83 s. The water behind the partition plate ($3.3 \leq x/B_w \leq 5.0$) oscillates in the downstream direction ($t$ = 0.27 s) and in the upstream one ($t$ = 0.83 s) alternately due to the effects of the strong vortex. Finally, the water in the wando is transported toward the main channel at $t$ = 1.17s. This suggests that the period $T$ of these semi-periodical behaviors of vortices is about 1.2 s.

In the case of E05, a vortex is observed in the zone of $0 \leq x/B_w \leq 1.7$. The strength of this vortex is much smaller than that of the case D05. The shape of this vortex is little different from a circle. This feature does not correspond to the case of C05 which has a symmetric shape to E05. This may be because the edge of the partition plate affects the flow direction at the wando junction ($z/B_w$ = 1.0).

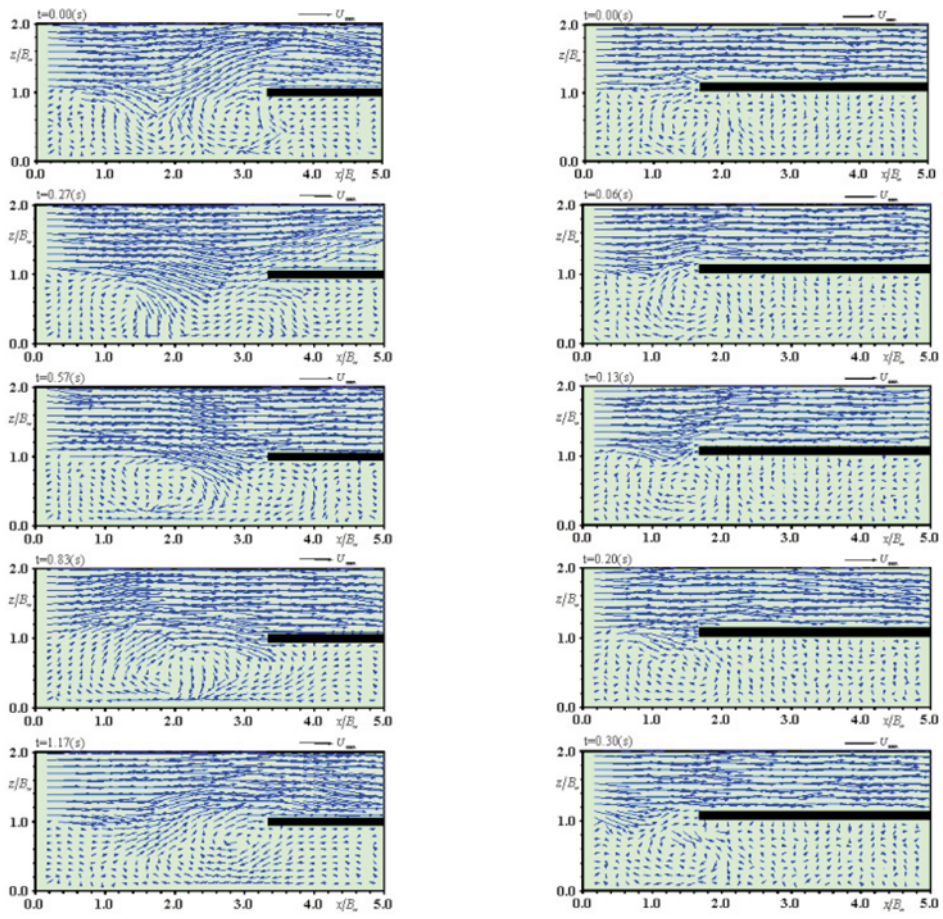


(d) case D05 (e) case E05

Fig. 5. Instaneous flow fields. (continued)

### *3.3 Variations of Free-Surface Fluctuations*

Figure 6 shows the variations of the free-surface fluctuations $\tilde{h}(t)$ at the points a, b and c for each case as shown in Fig. 3.

When the junction mouth is wide such as in B05 and D05, the amplitude of water-surface fluctuations at the point a (in wando) and c (in main channel) is quite large and the behavior of these fluctuations is semi-periodical. The shape of these time series is like a sine wave and out of phase. This means that when the free surface in the wando is rising, the free surface in the main channel is falling, and vice versa. In contrast, the variation of the free-surface fluctuations at the point b (junction) is somewhat complicated, because free-surface fluctuations at this point may be affected by both the wando and the main channel. The periods of the points a and c are the same as

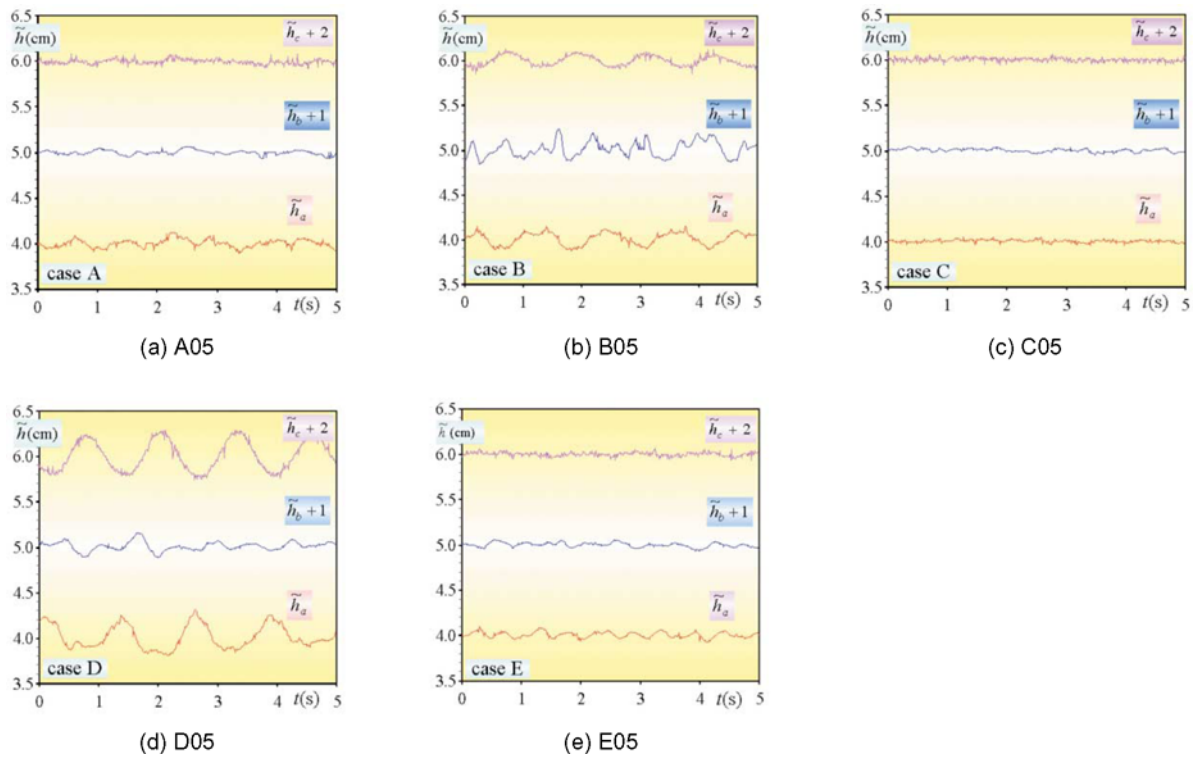


Fig. 6. Free surface fluctuations.

about 1.2 s. These values correspond to the period of vortices seen in Fig. 4 by eyes.

When the junction mouth is narrow such as in C05 and E05, the amplitudes of the fluctuations at the point b (junction) and c (in main channel) are small in comparison with those of cases B05 and D05.

### *3.4 FFT Analysis of Free-Surface Fluctuations*

Figure 7 shows the power spectrum $S(f)$ of the free-surface fluctuations calculated by FFT analysis. In the case of B05, large peaks of the spectrum can be seen at points a (in wando) and c (in main channel). However, there is no remarkable peak at point b (junction). On the other hand, peaks can be observed for all points in the case of D05. The strength of the peaks at points a and c is larger than that at point b. Therefore, it can be said that the water-surface fluctuations in the wando and main channel are periodical in comparison with those at the junction when the junction mouth is wide. The periods of these peaks (≈0.83 Hz = 1/1.2 s) correspond to those obtained from the behaviors of vortices in Fig. 4.

It was found that when the free surface in the wando is rising, the free surface in the main channel is falling and vice versa in such case that the junction mouth is wide. This period was about 1.2 s. It is well known that the seiche is generated in semi-closed open-channel flows. The period of the seiche $T_s$ is calculated by

$$T_s = \frac{2p}{\sqrt{2pg/l \cdot \tanh\left(2ph/l\right)}} \tag{1}$$

in which $l$ is a wave length. When $l$ is set to two times the channel width, the period of the seiche $T_s$ is 1.14 s in the present experiments. This value is almost the same as the value obtained from the FFT analysis. Therefore, it may be said that the behavior of the water-surface fluctuations is seiche when the junction mouth is wide. If this seiche theory is applied to actual rivers, e.g., the flow depth is 1 m and channel width is 50 m, a period of seiche is calculated to be about 1 minute.

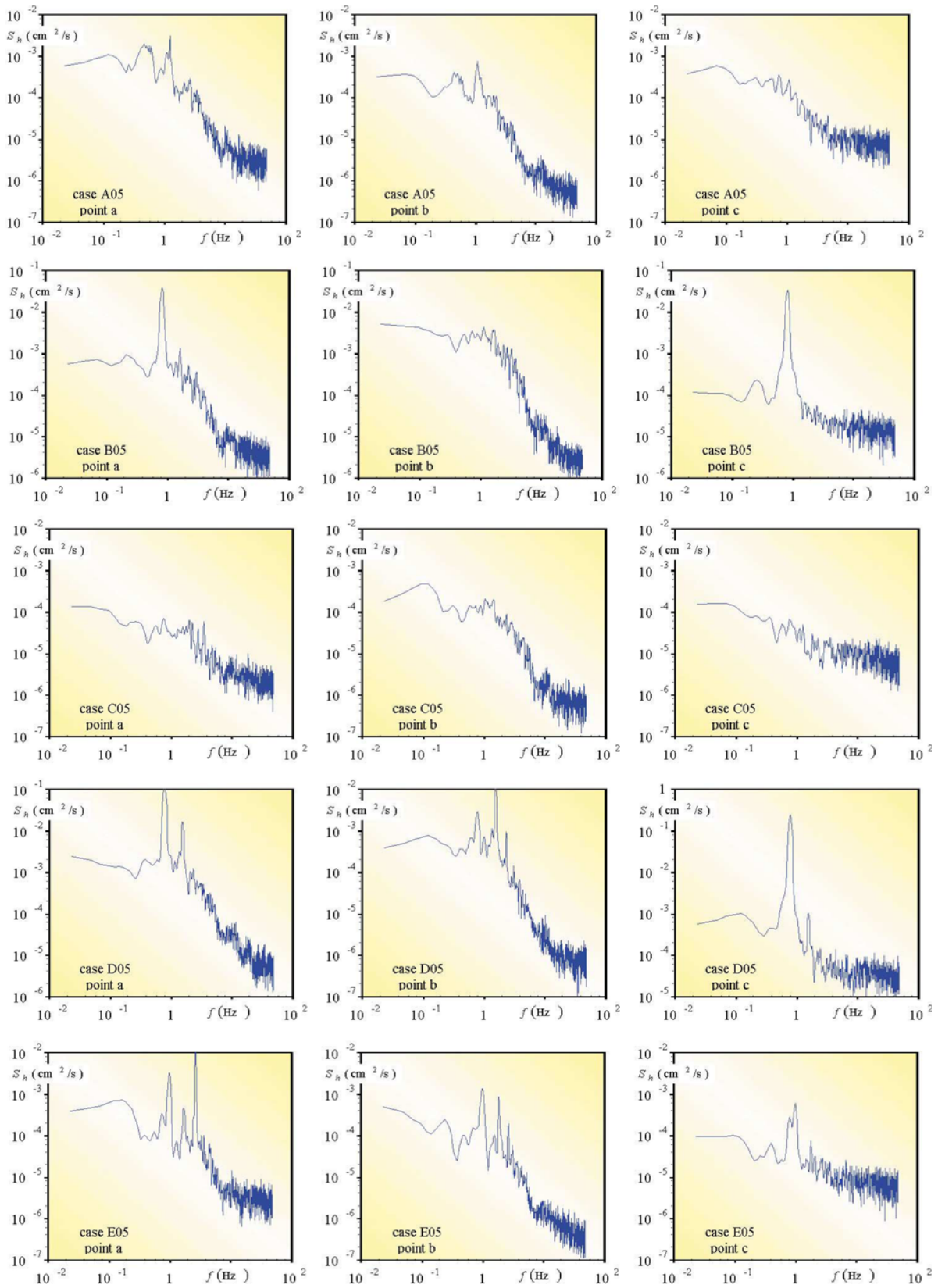


Fig. 7. Spectrum of free-surface fluctuations.

# 4. Conclusion

Five types of side-cavity "Wando" open-channel flows were built in a straight flume. The instantaneous flow velocities in a horizontal plane were measured accurately by using a PIV. Further, the free-surface fluctuations were measured by three sets of supersonic wave-gauges. It was found that a vortex, which is generated in the wando, is stable when the junction mouth between the wando and the main channel is narrow. In contrast, unstable vortices are generated semi-periodically when the junction mouth is wide. When the free surface in the wando is rising, its surface in the main channel is falling, and vice versa. It was found that this phenomenon is caused by a seiche.

## *Acknowledgments*

The financial support from the Foundation of River and Watershed Environment Management is gratefully acknowledged.

## *References*

Chen, F. and Ikeda, S., Annual J. of Hydraulic Eng., JSCE, Vol. 40, (1996), 787, (in Japanese).
Ikeda, S., Yoshike, T. and Sugimoto, T., Annual J. of Hydraulic Eng., JSCE, Vol. 43, (1999), 281, (in Japanese).
Kimura, I., Hosoda, T, Yasunaga, R. and Muramoto. Y., Annual J. of Hydraulic Eng., JSCE, Vol.41, (1997), 711, (in Japanese).
Muto, Y., Imamoto, H. and Ishigaki, T., Proc. of 12th Congress of APD-IAHR, Bangkok, Thailand, (2000), 353.
Nezu, I. and Onitsuka, K., 7th Int. Symp. on Flow Modeling and Turbulence Measurements, IAHR, Tainan, Taiwan, (1998), 109.
Nezu, I., Onitsuka, K., Iketani, K. and Takahashi, S., Proc. of 12th Congress of APD-IAHR, Bangkok, Thailand, (2000), 21.

## *Author Profile*

Iehisa Nezu: He received his B.E. (1971), M.E. (1973) and D.E. (Ph.D.) (1977) degrees from Kyoto University under the supervision of Professor H. Nakagawa. He stayed in Karlsruhe University in 1983 and collaborated with Professor W. Rodi. He was awarded "Thesis Prize" by JSCE(1976), "Karl Emil Hilgard Hydraulic Prize" by ASCE(1987) and "The Most Splendid Paper APD-IAHR Award" by IAHR(1998). His IAHR Monograph entitled "Turbulence in Open-Channel Flows", Balkema Pub.(1993) is well known in hydraulic community. He is a full professor and director of Hydraulics Laboratory in Kyoto University since 1996.

Kouki Onitsuka: He studied in Kyushu Institute of Technology (KIT) and received his Ph.D.(1997) degree under the supervision of Professor Masaru Ura from KIT, Japan. He is working as a research associate in the Department of Civil and Global Environment Engineering at Kyoto University under Professor Iehisa Nezu since 1997.